



# LUND UNIVERSITY

## Validation of an automated method to quantify stress-induced ischemia and infarction in rest-stress myocardial perfusion SPECT.

Fransson, Helen; Ljungberg, Michael; Carlsson, Marcus; Engblom, Henrik; Arheden, Håkan; Heiberg, Einar

*Published in:*  
Journal of Nuclear Cardiology

*DOI:*  
[10.1007/s12350-014-9863-y](https://doi.org/10.1007/s12350-014-9863-y)

2014

[Link to publication](#)

### *Citation for published version (APA):*

Fransson, H., Ljungberg, M., Carlsson, M., Engblom, H., Arheden, H., & Heiberg, E. (2014). Validation of an automated method to quantify stress-induced ischemia and infarction in rest-stress myocardial perfusion SPECT. *Journal of Nuclear Cardiology*, 21(3), 503-518. <https://doi.org/10.1007/s12350-014-9863-y>

*Total number of authors:*  
6

### **General rights**

Unless other specific re-use rights are stated the following general rights apply:  
Copyright and moral rights for the publications made accessible in the public portal are retained by the authors and/or other copyright owners and it is a condition of accessing publications that users recognise and abide by the legal requirements associated with these rights.

- Users may download and print one copy of any publication from the public portal for the purpose of private study or research.
- You may not further distribute the material or use it for any profit-making activity or commercial gain
- You may freely distribute the URL identifying the publication in the public portal

Read more about Creative commons licenses: <https://creativecommons.org/licenses/>

### **Take down policy**

If you believe that this document breaches copyright please contact us providing details, and we will remove access to the work immediately and investigate your claim.

LUND UNIVERSITY

PO Box 117  
221 00 Lund  
+46 46-222 00 00



1 **Title** Validation of an automated method to quantify stress-induced  
2 ischemia and infarction in rest-stress myocardial perfusion SPECT

3

4 **Authors** Helen Fransson<sup>1</sup>PhD, Michael Ljungberg<sup>2</sup>PhD, Marcus  
5 Carlsson<sup>1</sup>MD PhD, Henrik Engblom<sup>1</sup>MD PhD, Håkan Arheden<sup>1</sup>MD PhD,  
6 Einar Heiberg<sup>1</sup> PhD

7

8 **Author affiliation** <sup>1</sup>Department of Clinical Physiology and Nuclear  
9 Medicine, Lund University, Lund University Hospital, Sweden,

10 <sup>2</sup>Department of Medical Radiation Physics, Clinical Sciences, Lund, Lund  
11 University, Lund, Sweden

12

13 **Corresponding Author** Einar Heiberg, Department of Clinical Physiology,  
14 Lund University Hospital, SE-221 85 Lund, Sweden, Tel: +46-46-17 33 40  
15 Fax: +46-46-15 17 69, [einar.heiberg@med.lu.se](mailto:einar.heiberg@med.lu.se)

16

17 **Financial support** Swedish Heart Lung Foundation, Lund University  
18 Faculty of Medicine, the Swedish Research Council, Swedish Knowledge  
19 Foundation, and the Region of Scania.

1 **Abstract**

2 **Background:** Myocardial perfusion SPECT (MPS) is one of the frequently  
3 used methods for quantification of perfusion defects in patients with known  
4 or suspected coronary artery disease. This article describes open access  
5 software for automated quantification in MPS of stress-induced ischemia  
6 and infarction and provides phantom and in vivo validation.

7 **Methods and Results:** A total of 492 patients with known or suspected  
8 coronary artery disease underwent both stress and rest MPS. The proposed  
9 perfusion analysis algorithm (Segment) was trained in 140 patients and  
10 validated in the remaining 352 patients using visual scoring in MPS by an  
11 expert reader as reference standard. Furthermore, validation was performed  
12 with simulated perfusion defects in an anthropomorphic computer model.  
13 Total perfusion deficit (TPD, range 0-100), including both extent and  
14 severity of the perfusion defect, was used as the global measurement of the  
15 perfusion defects.

16 Mean bias±SD between TPD by Segment and the simulated TPD was  
17  $3.6\pm 3.8$  ( $R^2=0.92$ ). Mean bias±SD between TPD by Segment and the visual  
18 scoring in the patients was  $1.2\pm 2.9$  ( $R^2=0.64$ ) for stress-induced ischemia  
19 and  $-0.3\pm 3.1$  ( $R^2=0.86$ ) for infarction.

20 **Conclusion:** The proposed algorithm can detect and quantify perfusion  
21 defects in MPS with good agreement to expert readers and to simulated  
22 values in a computer phantom.

## 1 **Introduction**

2 Myocardial perfusion SPECT (MPS) is an established non-invasive imaging  
3 technique for detection and quantification of myocardial perfusion defects in  
4 patients with coronary artery disease (CAD) (1 , 2). Comparison of rest  
5 MPS to stress MPS enables quantification of stress-induced ischemia. By  
6 using normal limits of perfusion, MPS also provides the ability to quantify  
7 infarction (3). The interpretation of MPS images is routinely performed by  
8 visual reading supported by automated analysis software packages. The  
9 most common approach in current software packages to perform  
10 quantification of perfusion defects is to compare to a normal perfusion  
11 database (4-7). The comparison is traditionally performed for the rest and  
12 the stress tomographic sections separately, and thereafter the results are  
13 compared. One limitation with this approach is that no direct alignment of  
14 stress and rest MPS is performed. Another limitation is that the comparison  
15 depends on the two different left ventricular (LV) segmentations, which can  
16 differ significantly between the paired MPS images, in particular in the  
17 basal region of the LV. These limitations can confound the assessment of  
18 perfusion defects due to comparison of regions located in different parts of  
19 the myocardium. Furthermore, even when rest and stress tomographic  
20 sections are perfectly aligned, the comparison to normal limits is based on  
21 inter-patient comparison. This may cause true differences in perfusion to go  
22 undetected since the images are not compared directly.

1

2 A recent study has shown higher diagnostic performance for stress-induced  
3 ischemia by using voxel-based image registration and direct comparison of  
4 counts between rest and stress images, compared to the standard method of  
5 separate analysis of rest and stress images (8). Furthermore, incorporating  
6 regional myocardial function in automatic perfusion analysis has shown  
7 higher accuracy for detection of myocardial infarction compared to only  
8 including myocardial counts in the analysis (9). Therefore, the aim of this  
9 study was to combine voxel-based image registration of rest and stress  
10 images with regional myocardial function at rest to develop a new freeware  
11 method for quantification of both stress-induced ischemia and infarction in  
12 MPS images.

## 1 **Materials and Methods**

### 2 **Study population and design**

3 All patients provided written informed consent to participate in the study  
4 and the study was approved by the regional ethics committee. Patients  
5 referred for MPS imaging during 2008-2011, due to known or suspected  
6 coronary artery disease, with rest and stress MPS at the same day were  
7 considered for enrollment. A training set was designed by assessing the  
8 myocardial perfusion by experienced observers, and then include a control  
9 group of 90 patients with a normal perfusion scan and a CAD group of 50  
10 patients with perfusion defects. Inclusion criteria for the control group were  
11 normal global systolic function (Ejection fraction (EF) > 50). Exclusion  
12 criteria for the control group were history of CAD, atrial fibrillation,  
13 arrhythmia, LV bundle branch block, heart failure, pacemaker, death or  
14 valvular heart disease, within two years or prior to the MPS imaging. The  
15 remaining patients, both with and without perfusion defects, formed a test  
16 set of 352 patients. The patient characteristics for both the training set and  
17 the test set are shown in Table 1.

18

### 19 **Myocardial Perfusion SPECT Acquisition and Analysis**

20 Myocardial perfusion SPECT was performed according to established  
21 clinical one day protocols using a dual head camera GE Venti (GE  
22 Healthcare, Waukesha Wisconsin, USA). Gated MPS images were acquired

1 at stress and rest for each patient, after injection with  $^{99m}\text{Tc}$  tetrofosmin  
2 (Myoview, Amersham Health, Buckinghamshire, UK). Injection at stress  
3 was 4 MBq  $^{99m}\text{Tc}$  tetrofosmin per kg bodyweight, and at rest approximately  
4 12 MBq  $^{99m}\text{Tc}$  tetrofosmin per kg bodyweight. Patients were stressed using  
5 maximal exercise test, adenosine, or a combination of the two. Dobutamine  
6 was used when maximal exercise test and adenosine were contra-indicated.  
7 The patient was placed in supine position and imaged in steps of 3 degrees  
8 using a 64x64 matrix with a pixel size of 6.4x6.4 mm<sup>2</sup> and a slice thickness  
9 of 6.4 mm. Images were gated to a simultaneously acquired  
10 electrocardiogram using 8 frames per cardiac cycle. Image acquisition time  
11 was approximately 12 minutes. According to clinical practice at Lund  
12 University Hospital, iterative reconstruction using ordered subset  
13 expectation maximization (OSEM) with two iterations and ten subsets was  
14 performed with a low-pass Butterworth filter. For stress the cutoff frequency  
15 was set to 0.4 of Nyquist and an order of 10, and for rest the cutoff  
16 frequency was set to 0.52 of Nyquist and an order of 5. No attenuation or  
17 scatter correction was applied. Short-axis images were reconstructed semi-  
18 automatically with manual adjustments using the software package Cedars  
19 QGS/QPS (Xeleris version 3, GE Healthcare). Reconstructed MPS images  
20 were loaded into the software package Segment (version 1.9 Medviso AB,  
21 Lund, Sweden).  
22

1    **Computer Phantom Data**

2    As a complement to the patient validation, the automatic perfusion analysis  
3    algorithm was validated by simulated MPS images by a computer phantom.  
4    The simulated MPS projection data were generated by using the XCAT  
5    mathematical anthropomorphic phantom (10) together with the Monte Carlo  
6    based simulation program SIMIND (11). In the simulation, the SPECT  
7    system parameters were set according to the clinical one day protocol, as  
8    described above, and realistic noise levels were created by adding Poisson  
9    noise. Identical camera parameters were used to match as close as possible  
10   to realistic clinical situations. The simulation was performed in both male  
11   and female geometry, with varying LV geometries and varying sizes,  
12   location and severity of the perfusion defect. A total of 48 sets of  
13   tomographic sections (24 male, 24 female) were simulated, 12 with normal  
14   perfusion and 36 with various perfusion defects. The phantom projection  
15   data including effects from non-homogeneous photon attenuation, scatter  
16   and the collimator response, were reconstructed as described above for the  
17   patient data. Finally, the phantom data were loaded into the software  
18   packages Segment and QPS for automatic LV segmentation and perfusion  
19   analysis. Figure 1 shows one of the paired simulated MPS images with an  
20   overlaid LV segmentation by Segment.

21

22   **Visual Perfusion Scoring**

1 The manual perfusion analysis of the MPS images was performed in the  
2 software package Segment. The LV was automatically segmented as  
3 previously described (12), with manual corrections if necessary. The LV  
4 myocardia were automatically divided into 17 segments using the standard  
5 division of the LV (13), and each segment was scored manually for tracer  
6 uptake and presence of infarction, respectively. The manual interpretation to  
7 detect myocardial infarction using gated MPS was recently validated by  
8 cardiac magnetic resonance imaging, with high sensitivity and specificity  
9 for detecting infarction (14). Figure 2 illustrates the interface used in the  
10 scoring process. The scoring was performed by an experienced physician  
11 (MD, PhD) specialized in nuclear cardiology with 12 years of clinical and  
12 scientific experience with MPS. The observer was blinded to patient  
13 information and the results from the automatic perfusion analysis. To  
14 determine interobserver variability, two additional observers performed  
15 perfusion scoring in 40 MPS images, randomly chosen from the test set. The  
16 second and the third observer were blinded to the scoring by the first  
17 observer. The second and third observers are both experienced physicians  
18 (MD, PhD) specialized in nuclear cardiology with 10 and 20 years of  
19 experience with MPS, respectively.

20

21 A difference score was obtained by taking the difference between the stress  
22 and rest tracer uptake score in each of the 17 segments of the LV. Single

1 segments with a score of 1, which were not contiguous with segments of  
2 scores  $>0$ , were assigned a score of 0. By summation of the difference score  
3 a summed difference score (SDS) was obtained. Stress-induced ischemia  
4 was defined as a  $SDS \geq 2$ , as previously established (8). A summed rest  
5 score (SRS) was obtained by summation of the tracer uptake scores of those  
6 LV segments in the rest image where the infarct score was equal to 2.  
7 Myocardial infarction was defined by one or more regions with an infarct  
8 score of 2. For comparison with the automatic defect quantification, the  
9 summed scores were converted to percent of the total myocardium with  
10 defects by multiplying the summed scores by 100 and dividing by 64 (the  
11 maximum score). Those converted scores were labeled SD% and SR%, for  
12 stress-induced ischemia and infarction, respectively (15).

13

#### 14 **Automatic Perfusion Analysis**

15 The proposed algorithm for automatic perfusion analysis in MPS images is  
16 implemented in the freely available software Segment  
17 (<http://segment.heiberg.se>). In this study, Segment was used for both manual  
18 and automatic perfusion analysis (16). The LV was automatically  
19 segmented in both the gated and ungated tomographic sections as previously  
20 described (12), with manual corrections if necessary. The proposed  
21 automatic perfusion analysis algorithm then segments and quantifies the  
22 perfusion defects. The perfusion analysis algorithm starts by count

1 normalization and image registration of the ungated rest and stress  
2 tomographic sections. The normalization aims to normalize to similar  
3 maximum count in each image slice. The registration is an affine  
4 transformation aiming to have a direct comparison of voxels between the  
5 rest and the stress tomographic sections. The normalization and registration  
6 processes are described in more detail in the Appendix. Regional wall  
7 thickening was calculated from the LV segmentation in the rest gated  
8 tomographic sections, by increase in distance between computed LV walls.  
9 The wall thickening for each voxel was thereafter assigned to each  
10 myocardial voxel in the rest ungated tomographic sections. The rest and  
11 stress myocardial counts, the rest-stress counts change, and the rest wall  
12 thickening were used as features to classify the myocardium as normal,  
13 stress-induced ischemia or infarction, by a probabilistic classification  
14 algorithm. The classification was performed by a Naive Bayes classifier, as  
15 described in more detail in the Appendix. Finally, the perfusion defect  
16 segmentation was refined by considering *a priori* knowledge of perfusion  
17 defects propagation within the myocardium. The refinement of the perfusion  
18 segmentation is described in more detail in the Appendix. From the  
19 perfusion defect segmentation the perfusion defect was quantified by  
20 calculating the extent and total perfusion deficit (TPD) of the defect. Extent  
21 was presented as percentage of the LV. The TPD measure includes both  
22 extent and severity of the perfusion defect, and is a continuous value

1 ranging from 0 (no perfusion defect) to 100 (severe perfusion defect in the  
2 whole LV). TPD is calculated by(17)

$$TPD = 100 \times \frac{\sum_{i=0}^N score_i}{N}$$

3  
4 where  $N$  was the total number of voxels within the myocardium and  $score$   
5 was a continuous value assigned to each myocardial voxel ranging from 0  
6 (no defect) to 1 (severe defect). The TPD measurement for stress-induced  
7 ischemia was calculated by the count difference between stress and rest  
8 within the segmented stress-induced ischemia, and was labeled D-TPD. The  
9 TPD measurement for infarction was calculated for the segmented perfusion  
10 defect in the rest image and was labeled R-TPD.

11

## 12 **Perfusion Analysis by QPS**

13 For comparison, the MPS short-axis images were also loaded into the  
14 software package Quantitative Perfusion SPECT (QPS, version Suite2009;  
15 Cedars-Sinai Medical Centre, Los Angeles, CA) (15). The LV was  
16 automatically segmented by the program, with manual corrections of the LV  
17 segmentation when necessary. QPS then automatically quantifies the  
18 perfusion defect by TPD in the rest and stress tomographic sections  
19 separately using the vendor provided sex specific normal database. The  
20 TPD measurement for stress-induced ischemia was calculated by the  
21 difference between stress TPD and rest TPD (15), and labeled D-TPD. The

1 TPD measurement in the rest tomographic sections was used as assessment  
2 of infarction and labeled R-TPD.

3

#### 4 **Statistical analysis**

5 Values are presented as mean  $\pm$  SD unless otherwise stated. The diagnostic  
6 accuracy for TPD by Segment for detection of stress-induced ischemia and  
7 infarction, respectively, compared to visual scoring was obtained from  
8 analysis of receiver operating characteristic (ROC) curves (18). Sensitivity,  
9 specificity, accuracy as well as positive and negative predictive values with  
10 corresponding standard errors were calculated using standard definitions.

11 Inter-class correlation (ICC) was used for calculating interobserver  
12 variability. Pearson's linear regression analysis was performed to calculate  
13 the relationship between two data sets where normal distribution could be  
14 assumed. Student's paired t-test was performed to test statistical significance  
15 of differences between continuous variables. Differences with p-values  
16 below 0.05 were considered statistically significant. All statistical analyses  
17 except area under curve (AUC) calculation were performed in Matlab  
18 (R2011a, MathWorks). The AUC was calculated using SPSS (version 21,  
19 IBM Corporation).

## 1 **Results**

### 2 **Computer Phantom Study**

3 Figure 3 illustrates the relationship between the simulated TPD for the  
4 computer phantom and the TPD calculated by Segment and QPS. For the  
5 data sets with normal perfusion, 11 out of 12 studies were quantified as TPD  
6 = 0 by Segment, and 5 out of 12 studies were quantified as TPD = 0 by  
7 QPS.

8

### 9 **Patient Study**

10 The experts' classifications in the test set with 352 patients showed stress-  
11 induced ischemia and / or infarction in 38 % of the patients. Manual  
12 correction of the LV segmentation was performed in 5 % (18 out of 352) of  
13 the patients in the test set for Segment and 3 % (9 out of 352) for QPS.  
14 Interobserver variability between the three observers were for SR% ICC =  
15 0.97 and for SD% ICC = 0.77. The bias and SD between observer 1 and the  
16 two other observers are presented in Table 2. Figure 4 illustrates the  
17 relationship between the TPD calculated by Segment and the visual scoring.  
18 By excluding the wall thickening information in the automatic perfusion  
19 analysis in Segment, the bias between TPD calculated by Segment and the  
20 visual scoring was unchanged, compared to when the wall thickening  
21 information was included in the automatic analysis. Figure 5 illustrates the  
22 relationship between the TPD calculated by QPS and the visual scoring. For

1 the stress-induced ischemia quantification, the bias was not significantly  
2 different between Segment and QPS ( $p = 0.18$ ), whereas the variability was  
3 significantly lower for Segment than for QPS ( $p < 0.05$ ). For the infarct  
4 quantification, the bias and variability was significantly lower for Segment  
5 than for QPS ( $p < 0.05$ ). Figure 6 illustrates the distribution of the TPD  
6 measurement by the automatic analysis algorithms for patients with normal  
7 perfusion defined by the expert reader. For those patients with normal  
8 stress-rest difference perfusion ( $SD\% = 0$ ), Segment and QPS also assessed  
9  $D\text{-TPD} = 0$  in 48 % and 45 % of the cases, respectively. By using  $D\text{-TPD} <$   
10  $5$  (19) as the threshold for normal perfusion, Segment and QPS assessed  
11 normal perfusion in 90% and 86% of the cases, respectively. For those  
12 patients with normal rest perfusion ( $SR\% = 0$ ), Segment and QPS also  
13 assessed  $R\text{-TPD} = 0$  in 87 % and 14 % of the cases, respectively. By using  
14  $R\text{-TPD} < 5$  (19) as the threshold for normal perfusion, Segment and QPS  
15 assessed normal perfusion in 99% and 70% of the cases, respectively. Table  
16 2 presents the comparison of bias and variance for the two second observers  
17 and the two automatic algorithms, by using observer one as reference  
18 standard. Figure 7 illustrates the results from the image registration and  
19 perfusion defect segmentation by Segment in one patient with both stress-  
20 induced ischemia and infarction. Figure 8 shows the resulting ROC curves  
21 of diagnostic accuracy for TPD by Segment to detect stress-induced  
22 ischemia and infarction, respectively, when using manual scoring as

1 reference standard. The area under the curve was 0.87 to detect stress-  
2 induced ischemia, and 0.91 to detect infarction. The ROC curves of  
3 diagnostic accuracy for TPD by QPS to detect stress-induced ischemia and  
4 infarction, respectively, are found in Supplemental file 1. The area under the  
5 curve for QPS was 0.64 to detect stress-induced ischemia, and 0.89 to detect  
6 infarction. Table 3 present the result from the ROC analysis for both  
7 Segment and QPS.

## 1 **Discussion**

2 The major findings of this study was that the proposed perfusion analysis  
3 algorithm can detect and quantify stress-induced ischemia and infarction in  
4 MPS with good agreement to expert readers, in patients with varying  
5 degrees of stress-induced ischemia and infarction. Furthermore, the  
6 automatic perfusion defect quantification shows good agreement to  
7 simulated values by a computer phantom.

8

## 9 **Diagnostic performance**

10 The bias against expert readers was for infarct quantification lower for the  
11 proposed analysis algorithm in Segment than for QPS, see Figure 4 and 5.  
12 For stress-induced ischemia, the bias did not differ between the two  
13 automatic algorithms. For the patients with normal stress-rest difference  
14 perfusion, the two algorithms showed similar performance (left panels in  
15 Figure 6). For the patients with normal rest perfusion, however, Segment  
16 showed  $R\text{-TPD} = 0$  in 87% of the cases ( $R\text{-TPD} < 5$  in 99% of the cases)  
17 whereas QPS showed  $R\text{-TPD} = 0$  in only 14% of the cases ( $R\text{-TPD} < 5$  in  
18 70% of the cases), as shown in the right panels in Figure 6. As presented in  
19 Table 2, the automatic algorithms performance is comparable with the  
20 performance between observers.

21

1 The results of this study showed diagnostic performance similar to previous  
2 studies validating quantification of perfusion defects by automatic  
3 algorithms with manual interpretation of MPS images as reference standard  
4 (20-22). Lomsky et al. (20) reported a sensitivity and specificity for  
5 detection of stress-induced ischemia of 0.90 and 0.85, respectively, and for  
6 detection of infarction 0.89 and 0.96, respectively, for a patient population  
7 with ischemia in 17 % and infarction in 9 % of the patients. Garcia et al.  
8 (21) reported a sensitivity and specificity for detection of CAD of 0.83 and  
9 0.73, respectively, for a patient population with CAD in 73 % of the  
10 patients. Johansson et al. (22) evaluated three software packages for  
11 detection of CAD and reported an area under the curve of 0.87, 0.82 and  
12 0.76 and a sensitivity and specificity in the range of 0.79-0.87 and 0.42-  
13 0.79, respectively, for a patient population with CAD in 30 % of the  
14 patients. However, when comparing results from different studies, it is  
15 important to consider that the criteria used to determine diagnostic accuracy  
16 (sensitivity and specificity) are a function of the prevalence and severity of  
17 CAD in the population, which varied between the study populations above.  
18  
19 As showed by a previous study (23), detection of CAD with support by  
20 automatic perfusion analysis improved the consistency between observers.  
21 This illustrates one benefit with the support of automatic perfusion analysis,

1 since physicians may be able to use the second opinion from the automatic  
2 perfusion analysis to improve their clinical accuracy.

3

#### 4 **Computer Phantom Study**

5 The validation of the proposed automatic algorithm by the computer  
6 phantom showed good agreement with simulated values (Figure 3). Eleven  
7 of the twelve data sets with normal perfusion were correctly quantified as no  
8 perfusion defect by Segment. For QPS, five of the twelve normal data sets  
9 were correctly quantified as no perfusion defect. A slight overestimation of  
10 the perfusion defect was found for both of the automated algorithms.

11

#### 12 **Automatic Perfusion Algorithm**

13 The major algorithmic strengths of the developed method are 1)  
14 quantification of both stress-induced ischemia and infarction, 2) inclusion of  
15 regional myocardial function at rest to assess infarction, and 3) image  
16 registration enables direct comparison between rest and stress image data,  
17 making each person their own control. Image registration for MPS images  
18 has been applied previously for comparison to normal databases (6, 24) and  
19 for alignment of paired rest and stress images (8). The previous method (8)  
20 for alignment of paired rest and stress images performs a voxel-based co-  
21 registration, followed by comparison to a bullseye normal model of  
22 reversibility. However, this method only quantifies stress-induced ischemia

1 and does not quantify infarction. A method for quantification of both stress-  
2 induced ischemia and infarction was proposed by Lomsky et al. (20). This  
3 method uses an active shape model to segment the LV and obtain  
4 myocardial counts and regional myocardial function values. These values  
5 are then used as features in an artificial neural network to quantify perfusion  
6 defects. In this previous study, incorporation of regional myocardial  
7 function in the analysis resulted in higher accuracy for detection of  
8 infarction, compared to only include myocardial counts in the analysis (9).  
9 To our knowledge, the proposed method is the first method that combines  
10 voxel-based co-registration of rest and stress images, making each person  
11 their own control, with a probabilistic classification algorithm to quantify  
12 both stress-induced ischemia and infarction, the latter by considering both  
13 myocardial counts and regional myocardial function. Direct comparison of  
14 rest to stress after registration makes each person their own reference in the  
15 estimation of stress-induced ischemia. This is particularly advantageous  
16 when attenuation artifacts are present. Artifacts are usually present in both  
17 rest and stress MPS, and direct comparison will therefore improve the  
18 ability to distinguish ischemia from artifacts. Including wall thickening as a  
19 feature in the classification process was hypothesized to increase the  
20 specificity for defining infarction, by helping to distinguish infarction from  
21 artifacts (25, 26). For the patient material used in this study, the bias and  
22 variability between Segment and the visual analysis was unchanged,

1 regardless if the wall thickening information was included or not in the  
2 automatic analysis. In this study, the LV contour from the rest tomographic  
3 sections was used to define the LV myocardium in both the rest and the  
4 stress tomographic sections. The rest LV contour was hypothesized to be of  
5 higher quality than the stress LV contour, due to influence from potential  
6 stress-induced ischemia. This is opposite from the rest-stress analysis  
7 algorithm presented by Prasad et al. (8), where the stress contour was used  
8 to define the LV myocardium.

9

#### 10 **Study Limitations**

11 One limitation with the proposed perfusion analysis algorithm is that it uses  
12 an affine transformation, without scaling, of the stress tomographic sections  
13 in the co-registration with the rest tomographic sections. This could  
14 potentially be an issue in patients with significant post-ischemic LV  
15 dilatation after stress when manual adjustment in the co-registration might  
16 be required. No patients in the present study needed manual correction in  
17 the co-registration. Another limitation is that this study only included MPS  
18 data generated by one camera setting and image reconstruction method.  
19 Further validation is necessary to investigate the performance of the  
20 proposed algorithm for other camera settings and reconstruction methods. In  
21 this study, we used expert readers as reference standard, and not an analysis  
22 method independent of MPS, like coronary angiography or PET. However,

- 1 the aim of the algorithm is to emulate the manual interpretation of
- 2 myocardial perfusion analysis by MPS, and to provide support to physicians
- 3 reporting MPS studies.

1 **Conclusions**

2 The proposed algorithm can detect and quantify stress-induced ischemia and  
3 infarction in MPS with good agreement to expert readers, and quantify  
4 stress-induced ischemia with good agreement to simulated values by a  
5 computer phantom. Hence, the proposed algorithm shows potential to  
6 provide clinically relevant quantification of perfusion defects by MPS.

1 **Acknowledgements**

2 The authors would like to thank technicians at Department of Clinical  
3 Physiology at Skåne University Hospital in Lund for invaluable help with  
4 data acquisition, and Shahnaz Akil for help with data analysis. Financial  
5 support was provided by Swedish Heart Lung Foundation, Lund University  
6 Faculty of Medicine, the Swedish Research Council (grant 2008-2461,  
7 2008-2949, 2012-4944), Swedish Knowledge Foundation (grant 2009-  
8 0080), and Region of Scania.

## 1 **Appendix**

### 2 **Automatic Perfusion Algorithm**

#### 3 *Count Normalization*

4 The count normalization aims to compensate for both the underestimated  
5 counts in the basal and apical part of the LV (due to thinner myocardial wall  
6 in these regions), as well as the relative nature of the counts in MPS images.  
7 The compensation method used here has been used before in an algorithm  
8 for quantification of myocardium at risk in MPS (17). The underestimation  
9 of counts in the basal part of the LV was compensated in each basal slice,  
10 defined as the slices with outflow tract by the LV segmentation. The  
11 compensation was performed by normalization of the highest count in the  
12 myocardium in each basal slice to the highest count in the whole LV  
13 myocardium. The normalization factor for the apex was calculated as the  
14 mean of the normalization factors in the two most basal slices. The apex  
15 cannot be used to set the normalization factor since apical defects might  
16 result in complete absence of counts in the apex. The relative nature of the  
17 counts in MPS images was compensated by normalization to the maximum  
18 count within the LV myocardium for each set of tomographic sections.

19

#### 20 *Image Registration*

21 As a first step in the image registration process, the LV contours were used  
22 to place the stress image LV center at the rest image LV center. Iterative

1 image registration was then performed using the Simplex optimization  
2 algorithm (27). The iterative registration algorithm is based on  
3 maximization of the normalized mutual information (NMI) between the rest  
4 and the stress tomographic sections by performing an affine 3-dimensional  
5 transformation of the stress image. The transformation includes six  
6 parameters, three for translation and three for rotation of the stress  
7 tomographic sections. The NMI measures the mutual dependence of two  
8 variables and is described by Studholme et al. (28). In short, the NMI  
9 calculation starts by grouping the counts in each set of tomographic sections  
10 into bins and then calculating the NMI from the similarity between  
11 corresponding voxel counts and the occurrence of the grouped bins. In this  
12 study, the image counts for each set of tomographic sections were grouped  
13 into 50 bins according to their values.

14

#### 15 *Training of the Classification Algorithm*

16 The training of the classification algorithm started by count normalization  
17 and image registration of the rest and the stress image stacks, for the  
18 patients in the training set. This was followed by determination of four  
19 myocardial features; rest and stress counts, rest-stress count change, and rest  
20 wall thickening, for each myocardial voxel. The rest wall thickening was  
21 calculated in the gated rest image stack and by interpolation assign to each  
22 ungated myocardial voxel. Thereafter, each voxel was assigned to one of the

1 three classes; normal myocardium, stress-induced ischemia or infarction.  
2 The class assignment was performed by interpolating the visual scoring  
3 values over the myocardium and assigning the voxels with a rest-stress  
4 difference score greater than 1 as stress-induced ischemia, and the voxels  
5 with an infarct score greater than 1 as infarction. The myocardial features  
6 together with the class identity, determined by the expert reader, were used  
7 as input to the training of the classification algorithm. The classification  
8 algorithm was a Naive Bayes classifier, which are based on applying Bayes'  
9 theorem with strong independence assumptions. The parameters estimated  
10 during the training were the class prior probabilities,  $p(C)$ , and the  
11 probability distributions,  $p(F/C)$ , where  $F$  are the features and  $C$  the classes.  
12 These parameters were then used in the segmentation of the perfusion  
13 defects in the test set, as described in the next section.

14

#### 15 *Classification algorithm*

16 The measured values of the features were used to classify each myocardial  
17 voxel by the Naive Bayes classifier into one of three classes; normal, stress-  
18 induced ischemia or infarction. The classification was performed by  
19 calculating the three class probabilities for each voxel by

$$p(C_i|F_1, \dots, F_n) = p(C_i) \prod_{j=1}^n p(F_j|C_i)$$

20

1 where  $n$  is the number of features and  $i$  is the class number. The values of  
2  $p(C)$  and  $p(F/C)$  derives from the training of the classifier. From the  
3 probabilities, the perfusion defect segmentation was performed by assign  
4 each myocardial voxel to the class with the highest computed probability.

5

#### 6 *Refinement of the segmentation*

7 The perfusion defect segmentation derived from the probabilistic  
8 classification was then refined based on *a priori* knowledge of perfusion  
9 defect propagations, established in a previous study (17), as follows.

10 Segmented regions with a volume less than 5 % of the LV were considered  
11 to be noise and removed from the segmentation. Regions in the myocardium  
12 less than 1 cm<sup>2</sup> in a short-axis slice, which were completely surrounded by  
13 voxels included in the segmentation, were made part of the segmented  
14 region. Any region that did not approach the endocardium, as determined by  
15 the centerline method (29), were filled in the endocardial direction, based on  
16 the expected propagation of perfusion defects from endocardium to  
17 epicardium.

## 1 References

- 2 (1) Sciagra R, Leoncini M. Gated single-photon emission computed  
3 tomography. The present-day "one-stop-shop" for cardiac imaging.  
4 Q J Nucl Med Mol Imaging 2005;49:19-29.
- 5 (2) Underwood SR, Anagnostopoulos C, Cerqueira M, Ell PJ, Flint EJ,  
6 Harbinson M et al. Myocardial perfusion scintigraphy: the evidence.  
7 European journal of nuclear medicine and molecular imaging  
8 2004;31:261-91.
- 9 (3) Gibbons RJ, Miller TD, Christian TF. Infarct size measured by  
10 single photon emission computed tomographic imaging with  
11 (99m)Tc-sestamibi: A measure of the efficacy of therapy in acute  
12 myocardial infarction. Circulation 2000;101:101-8.
- 13 (4) Itti E, Klein G, Rosso J, Evangelista E, Monin JL, Gueret P et al.  
14 Assessment of myocardial reperfusion after myocardial infarction  
15 using automatic 3-dimensional quantification and template  
16 matching. J Nucl Med 2004;45:1981-8.
- 17 (5) Okuda K, Nakajima K, Hosoya T, Ishikawa T, Matsuo S, Kawano M  
18 et al. Quantification of myocardial perfusion SPECT using freeware  
19 package (cardioBull). Annals of nuclear medicine 2011;25:571-9.
- 20 (6) Slomka PJ, Hurwitz GA, Stephenson J, Craddock T. Automated  
21 alignment and sizing of myocardial stress and rest scans to three-  
22 dimensional normal templates using an image registration algorithm.  
23 J Nucl Med 1995;36:1115-22.
- 24 (7) Slomka PJ, Nishina H, Berman DS, Akincioglu C, Abidov A,  
25 Friedman JD et al. Automated quantification of myocardial  
26 perfusion SPECT using simplified normal limits. J Nucl Cardiol  
27 2005;12:66-77.
- 28 (8) Prasad M, Slomka PJ, Fish M, Kavanagh P, Gerlach J, Hayes S et al.  
29 Improved quantification and normal limits for myocardial perfusion  
30 stress-rest change. J Nucl Med 2010;51:204-9.
- 31 (9) Gjerdtsson P, Lomsky M, Richter J, Ohlsson M, Tout D, van  
32 Aswegen A et al. The added value of ECG-gating for the diagnosis  
33 of myocardial infarction using myocardial perfusion scintigraphy  
34 and artificial neural networks. Clinical physiology and functional  
35 imaging 2006;26:301-4.
- 36 (10) Segars WP, Sturgeon G, Mendonca S, Grimes J, Tsui BM. 4D  
37 XCAT phantom for multimodality imaging research. Medical  
38 physics 2010;37:4902-15.
- 39 (11) Ljungberg M, Strand SE. A Monte Carlo program for the simulation  
40 of scintillation camera characteristics. Comput Methods Programs  
41 Biomed 1989;29:257-72.
- 42 (12) Sonesson H, Hedeer F, Arevalo C, Carlsson M, Engblom H, Ubachs  
43 JF et al. Development and validation of a new automatic algorithm

- 1 for quantification of left ventricular volumes and function in gated  
2 myocardial perfusion SPECT using cardiac magnetic resonance as  
3 reference standard. *J Nucl Cardiol* 2011;18:874-85.
- 4 (13) Cerqueira MD, Weissman NJ, Dilsizian V, Jacobs AK, Kaul S,  
5 Laskey WK et al. Standardized myocardial segmentation and  
6 nomenclature for tomographic imaging of the heart: a statement for  
7 healthcare professionals from the Cardiac Imaging Committee of the  
8 Council on Clinical Cardiology of the American Heart Association.  
9 *Circulation* 2002;105:539-42.
- 10 (14) Carlsson M, Hedeer F, Engblom H, Arheden H. Head-to-head  
11 comparison of a 2-day myocardial perfusion gated SPECT protocol  
12 and cardiac magnetic resonance late gadolinium enhancement for the  
13 detection of myocardial infarction. *J Nucl Cardiol* 2013.
- 14 (15) Germano G, Kavanagh PB, Slomka PJ, Van Kriekinge SD, Pollard  
15 G, Berman DS. Quantitation in gated perfusion SPECT imaging: the  
16 Cedars-Sinai approach. *J Nucl Cardiol* 2007;14:433-54.
- 17 (16) Heiberg E, Sjogren J, Ugander M, Carlsson M, Engblom H, Arheden  
18 H. Design and validation of Segment - freely available software for  
19 cardiovascular image analysis. *BMC Med Imaging* 2010;10:1.
- 20 (17) Sonesson H, Engblom H, Hedstrom E, Bouvier F, Sorensson P,  
21 Pernow J et al. An automatic method for quantification of  
22 myocardium at risk from myocardial perfusion SPECT in patients  
23 with acute coronary occlusion. *J Nucl Cardiol* 2010;17:831-40.
- 24 (18) Altman DG, Bland JM. Diagnostic tests 3: receiver operating  
25 characteristic plots. *BMJ (Clinical research ed)* 1994;309:188.
- 26 (19) Berman DS, Kang X, Slomka PJ, Gerlach J, de Yang L, Hayes SW  
27 et al. Underestimation of extent of ischemia by gated SPECT  
28 myocardial perfusion imaging in patients with left main coronary  
29 artery disease. *J Nucl Cardiol* 2007;14:521-8.
- 30 (20) Lomsky M, Gjertsson P, Johansson L, Richter J, Ohlsson M, Tout D  
31 et al. Evaluation of a decision support system for interpretation of  
32 myocardial perfusion gated SPECT. *European journal of nuclear  
33 medicine and molecular imaging* 2008;35:1523-9.
- 34 (21) Garcia EV, Cooke CD, Folks RD, Santana CA, Krawczynska EG,  
35 De Braal L et al. Diagnostic performance of an expert system for the  
36 interpretation of myocardial perfusion SPECT studies. *J Nucl Med*  
37 2001;42:1185-91.
- 38 (22) Johansson L, Lomsky M, Marving J, Ohlsson M, Svensson SE,  
39 Edenbrandt L. Diagnostic evaluation of three cardiac software  
40 packages using a consecutive group of patients. *EJNMMI research*  
41 2011;1:22.
- 42 (23) Lindahl D, Lanke J, Lundin A, Palmer J, Edenbrandt L. Improved  
43 classifications of myocardial bull's-eye scintigrams with computer-  
44 based decision support system. *J Nucl Med* 1999;40:96-101.

- 1 (24) Declerck J, Feldmar J, Goris ML, Betting F. Automatic registration  
2 and alignment on a template of cardiac stress and rest reoriented  
3 SPECT images. IEEE transactions on medical imaging 1997;16:727-  
4 37.
- 5 (25) DePuey EG, Rozanski A. Using gated technetium-99m-sestamibi  
6 SPECT to characterize fixed myocardial defects as infarct or artifact.  
7 J Nucl Med 1995;36:952-5.
- 8 (26) Fleischmann S, Koepfli P, Namdar M, Wyss CA, Jenni R,  
9 Kaufmann PA. Gated (99m)Tc-tetrofosmin SPECT for  
10 discriminating infarct from artifact in fixed myocardial perfusion  
11 defects. J Nucl Med 2004;45:754-9.
- 12 (27) Cardoso MF, Salcedo RL, de Azevedo SF. The simplex-simulated  
13 annealing approach to continuous non-linear optimization. Comput  
14 Chem Eng 1996;20:1065-80.
- 15 (28) Studholme C, Hill DLG, Hawkes DJ. An overlap invariant entropy  
16 measure of 3D medical image alignment. Pattern Recogn  
17 1999;32:71-86.
- 18 (29) Sheehan FH, Bolson EL, Dodge HT, Mathey DG, Schofer J, Woo  
19 HW. Advantages and applications of the centerline method for  
20 characterizing regional ventricular function. Circulation  
21 1986;74:293-305.  
22  
23

1 **TABLE 1**

	Training set		Test set
	Controls	CAD group	
Number of patients	90	50	352
Age (year)	60 ± 9	69 ± 9	66 ± 10
Gender (men / women)	45 / 45	25 / 25	180 / 172
LVM (g)	121 ± 21	139 ± 34	133 ± 34
EDV (ml)	141 ± 33	162 ± 65	159 ± 64
ESV (ml)	53 ± 17	79 ± 55	74 ± 56
EF (%)	63 ± 7	55 ± 13	57 ± 12
SDS ≥ 2 (%)	0	82	23
SDS LAD ≥ 2 (%)	0	52	16
SDS RCA ≥ 2 (%)	0	44	13
SDS LCx ≥ 2 (%)	0	18	6
Infarct score ≥ 2 (%)	0	52	20
Infarct score LAD ≥ 2 (%)	0	20	13
Infarct score RCA ≥ 2 (%)	0	44	13
Infarct score LCx ≥ 2 (%)	0	24	5

2

3 **TABLE 1 Patient characteristics.**

4 The LVM, EDV, ESV and EF were derived from the automatic LV

5 segmentation, and the summed scores were generated by visual scoring.

6 LVM = left ventricular mass, EDV = end-diastolic volume, ESV = end-

7 systolic volume, EF = ejection fraction, SDS = summed difference score,

8 LAD = left anterior descending artery, LCx = left circumflex artery, RCA =

9 right coronary artery

1 **TABLE 2**

	<b>Stress-induced ischemia</b>	<b>Infarction</b>
Observer 2	2.7 ± 3.9	0.3 ± 2.9
Observer 3	3.0 ± 4.1	0.0 ± 1.6
Segment	0.7 ± 3.8	-1.3 ± 4.7
QPS	0.1 ± 5.8	3.1 ± 3.8

2

3 **TABLE 2 Validation**

4 Bias ± SD against the reference standard of visual analysis of an expert  
5 reader for the subpopulation of 40 patients included in the interobserver  
6 analysis. Note that the results by the automated algorithms, Segment and  
7 QPS, are in the same range as the interobserver variability.

1 **TABLE 3**

2

	<b>Stress-induced ischemia</b>					
	<b>Segment</b>			<b>QPS</b>		
	<b>All</b>	<b>Men</b>	<b>Women</b>	<b>All</b>	<b>Men</b>	<b>Women</b>
Threshold	3.4	3.4	2.2	2.0	1.0	3.0
Sensitivity	0.76 (0.047)	0.82 (0.057)	0.76 (0.071)	0.55 (0.055)	0.60 (0.073)	0.49 (0.082)
Specificity	0.83 (0.023)	0.82 (0.033)	0.78 (0.036)	0.69 (0.028)	0.69 (0.040)	0.68 (0.040)
Positive predictive value	0.58 (0.048)	0.61 (0.063)	0.48 (0.066)	0.35 (0.042)	0.39 (0.059)	0.30 (0.058)
Negative predictive value	0.92 (0.017)	0.93 (0.023)	0.92 (0.025)	0.83 (0.025)	0.84 (0.035)	0.83 (0.036)
Accuracy	0.82 (0.021)	0.82 (0.028)	0.77 (0.032)	0.66 (0.025)	0.67 (0.035)	0.64 (0.037)
True positive fraction	0.18 (0.020)	0.21 (0.030)	0.16 (0.028)	0.13 (0.018)	0.15 (0.027)	0.10 (0.023)
False positive fraction	0.13 (0.018)	0.13 (0.025)	0.17 (0.029)	0.24 (0.023)	0.23 (0.032)	0.25 (0.033)
True negative fraction	0.64 (0.026)	0.62 (0.036)	0.61 (0.037)	0.53 (0.027)	0.52 (0.037)	0.53 (0.038)
False negative fraction	0.06 (0.012)	0.04 (0.015)	0.05 (0.017)	0.11 (0.016)	0.10 (0.022)	0.11 (0.024)

	<b>Infarction</b>					
	<b>Segment</b>			<b>QPS</b>		
	<b>All</b>	<b>Men</b>	<b>Women</b>	<b>All</b>	<b>Men</b>	<b>Women</b>
Threshold	1.2	1.2	1.7	6.0	6.0	6.0
Sensitivity	0.86 (0.039)	0.87 (0.047)	0.84 (0.073)	0.82 (0.043)	0.81 (0.054)	0.84 (0.073)
Specificity	0.93 (0.016)	0.91 (0.025)	0.95 (0.018)	0.84 (0.022)	0.82 (0.034)	0.86 (0.029)
Positive predictive value	0.77 (0.045)	0.81 (0.052)	0.75 (0.082)	0.59 (0.047)	0.65 (0.059)	0.50 (0.077)
Negative predictive value	0.96 (0.012)	0.94 (0.021)	0.97 (0.014)	0.94 (0.015)	0.91 (0.026)	0.97 (0.015)
Accuracy	0.91 (0.015)	0.90 (0.022)	0.94 (0.019)	0.84 (0.020)	0.82 (0.029)	0.85 (0.027)
True positive fraction	0.19 (0.021)	0.26 (0.033)	0.12 (0.025)	0.18 (0.021)	0.24 (0.032)	0.12 (0.025)
False positive fraction	0.06 (0.012)	0.06 (0.018)	0.04 (0.015)	0.13 (0.018)	0.13 (0.025)	0.12 (0.025)
True negative fraction	0.72 (0.024)	0.64 (0.036)	0.81 (0.030)	0.65 (0.025)	0.58 (0.037)	0.73 (0.034)
False negative fraction	0.03 (0.009)	0.04 (0.014)	0.02 (0.011)	0.04 (0.010)	0.06 (0.017)	0.02 (0.011)

3

4 **TABLE 3 ROC analysis**

5 Result from the ROC analysis for the both automatic perfusion analysis

6 algorithms Segment and QPS, by using expert reader as reference standard.

7 The values in parentheses indicate the standard error.

**FIGURE 1:** The simulated MPS in female geometry with a perfusion defect in the RCA region in the stress image. The yellow arrows indicate the perfusion defect with a severity of 40 %. The white lines indicate the LV contours derived from automatic segmentation by Segment.

**FIGURE 2:** Illustration of the interface for manual scoring of tracer uptake (A) and presence of infarct (B). In the scoring process, three short-axis (basal, midventricular and apical) and two long-axis (horizontal and vertical) tomographic sections were shown with the 17 segment model overlaid. For the scoring of tracer uptake, the ungated rest and stress tomographic sections were used, and for the scoring of presence of infarction, the gated and ungated rest tomographic sections were used. The tracer uptake in each segment was graded using a 5-point scale (0 = normal, 1 = equivocal, 2 = moderate, 3 = severe reduction, and 4 = apparent absence). The presence of infarction was graded using a 3-point scale (0 = normal, 1 = equivocal and 2 = infarction/hibernation).

**FIGURE 3:** Relationship between the simulated TPD by the computer phantom and the D-TPD measured by Segment (upper panels) and QPS (lower panels). In the left panels the dashed line is the line of identity, and the solid line is the linear regression line. In the right panels the solid line is the mean bias and the dashed lines 2 SD. Please note some symbols have been superimposed.

D-TPD = difference total perfusion deficit

**FIGURE 4:** Relationship between visual scoring by the expert reader and perfusion defect quantification by Segment. In the left panel the solid line is the linear regression line. In the

right panel the solid line is the mean bias and the dashed lines 2 SD. Please note some symbols have been superimposed.

SD%, SR% = visual perfusion scoring for stress-induced ischemia and infarction, respectively, D-TPD, R-TPD = total perfusion deficit for stress-induced ischemia and infarction, respectively

**FIGURE 5:** Relationship between visual scoring by the expert reader and perfusion defect quantification by QPS. In the left panel the solid line is the linear regression line. In the right panel the solid line is the mean bias and the dashed lines 2 SD. Please note some symbols have been superimposed.

SD%, SR% = visual perfusion scoring for stress-induced ischemia and infarction, respectively, D-TPD, R-TPD = total perfusion deficit for stress-induced ischemia and infarction, respectively

**FIGURE 6:** The upper left panel shows the distribution of the TPD quantification by Segment for the patients with normal myocardial perfusion for stress-rest difference by the expert reader (SD% = 0). The upper right panel shows the distribution of the TPD quantification by Segment for the patients with normal myocardial perfusion at rest by the expert reader (SR% = 0). The lower panels show the corresponding plots for the TPD quantification by QPS.

TPD = total perfusion deficit, SD%, SR% = visual perfusion scoring for stress-induced ischemia and infarction, respectively

**FIGURE 7:** Results from the image registration and perfusion defect quantification by Segment in one patient with both stress-induced ischemia and infarction. The white lines

indicate the LV segmentation derived from the rest tomographic sections and transferred to the aligned stress image. The yellow lines indicate the perfusion defect segmentation. Stress-induced ischemia was measured to D-TPD = 11 by Segment and SD% = 14 by the expert reader. Infarction was measured to R-TPD = 4 by Segment and SR% = 5 by the expert reader. SD%, SR% = visual perfusion scoring for stress-induced ischemia and infarction, respectively, D-TPD, R-TPD = total perfusion deficit for stress-induced ischemia and infarction, respectively

**FIGURE 8:** ROC curve of diagnostic accuracy for TPD by Segments to detect stress-induced ischemia and infarction, respectively, compared to the reference standard visual scoring by the expert reader. The blue circles indicate the point on the ROC curve closest to the upper left corner, and the corresponding TPD threshold and statistical analysis results are presented in Table 3. The values in parentheses indicate the standard error of the AUC.

TPD = total perfusion deficit, AUC = area under curve

**SUPPLEMENTAL FIGURE 1:** ROC curve of diagnostic accuracy for TPD by QPS to detect stress-induced ischemia and infarction, respectively, compared to the reference standard visual scoring by the expert reader. The blue circles indicate the point on the ROC curve closest to the upper left corner, and the corresponding TPD threshold and statistical analysis results are presented in Table 3. The values in parentheses indicate the standard error of the AUC.

TPD = total perfusion deficit, AUC = area under curve

# Stress

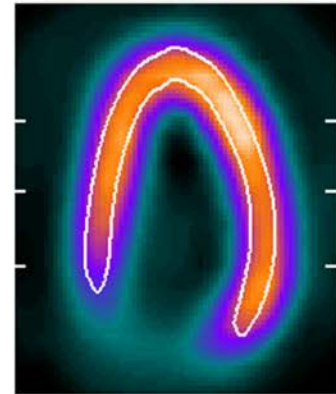
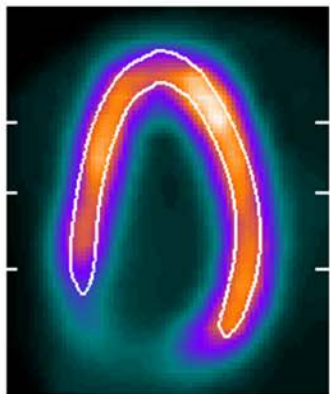
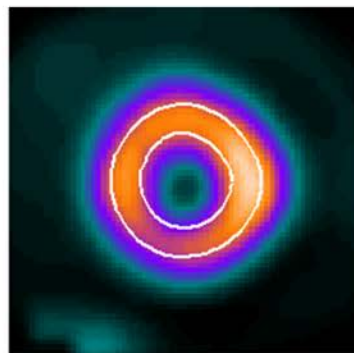
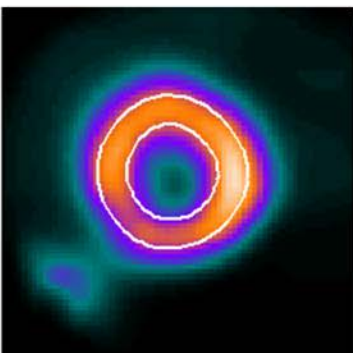
# Rest

Apical SA

Apical SA

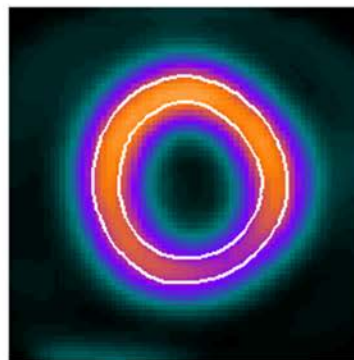
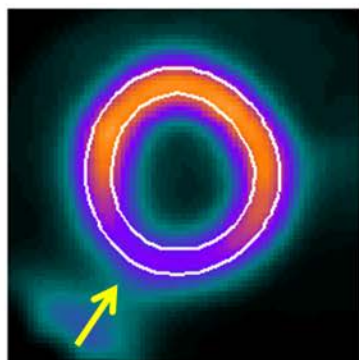
HLA

HLA



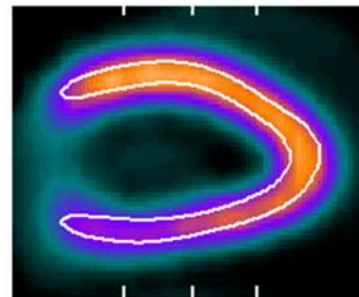
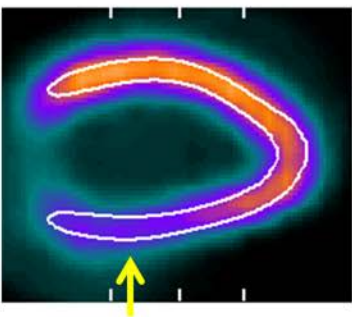
Midventricular SA

Midventricular SA



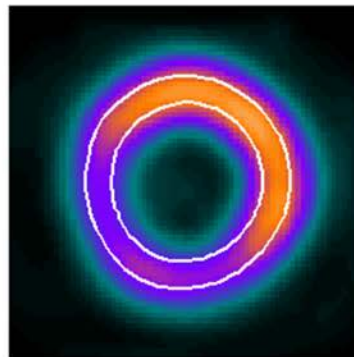
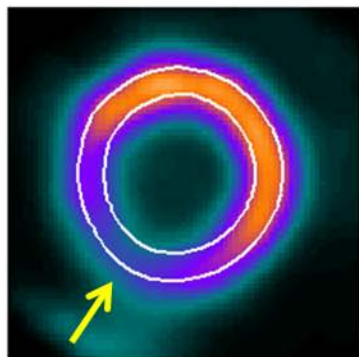
VLA

VLA

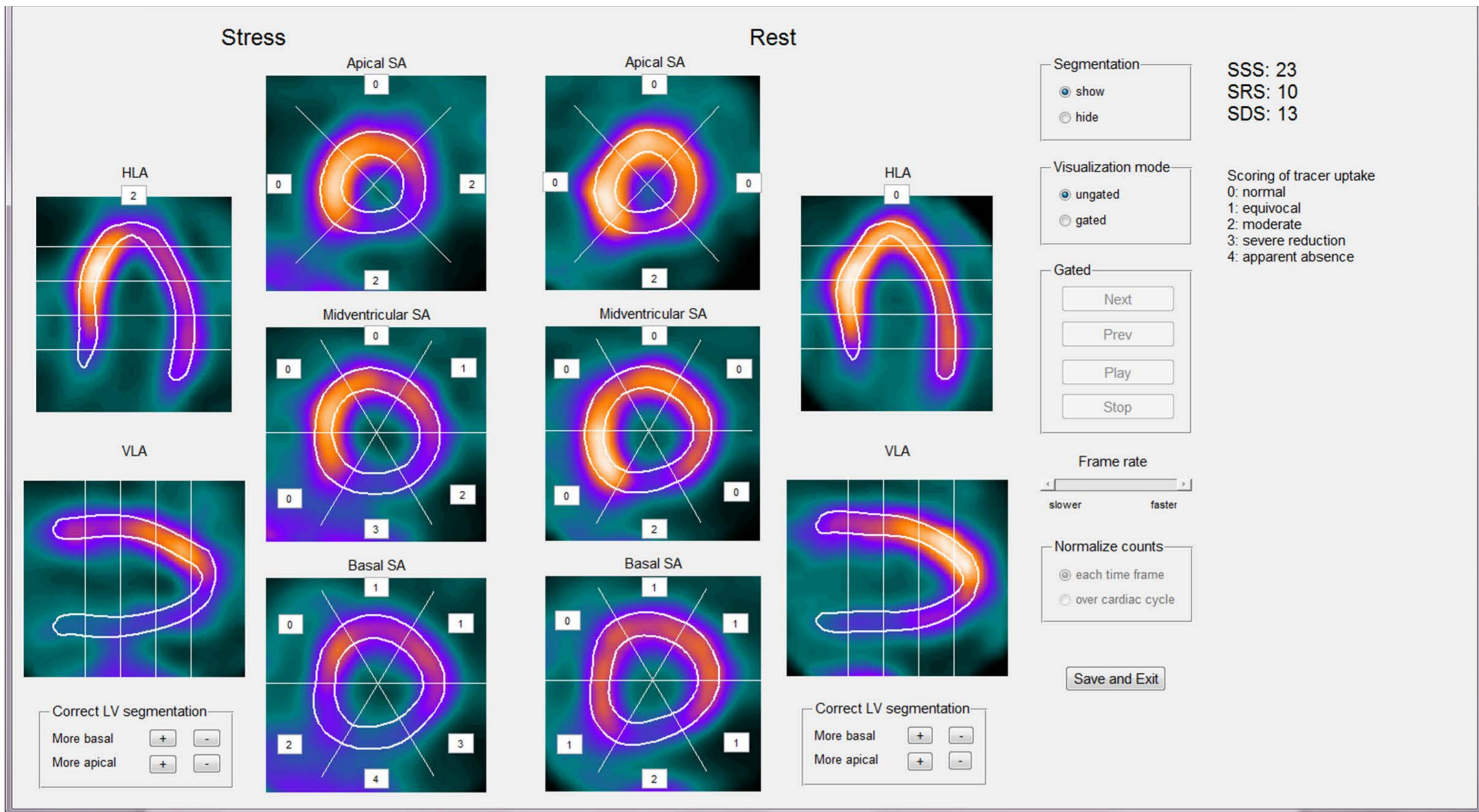


Basal SA

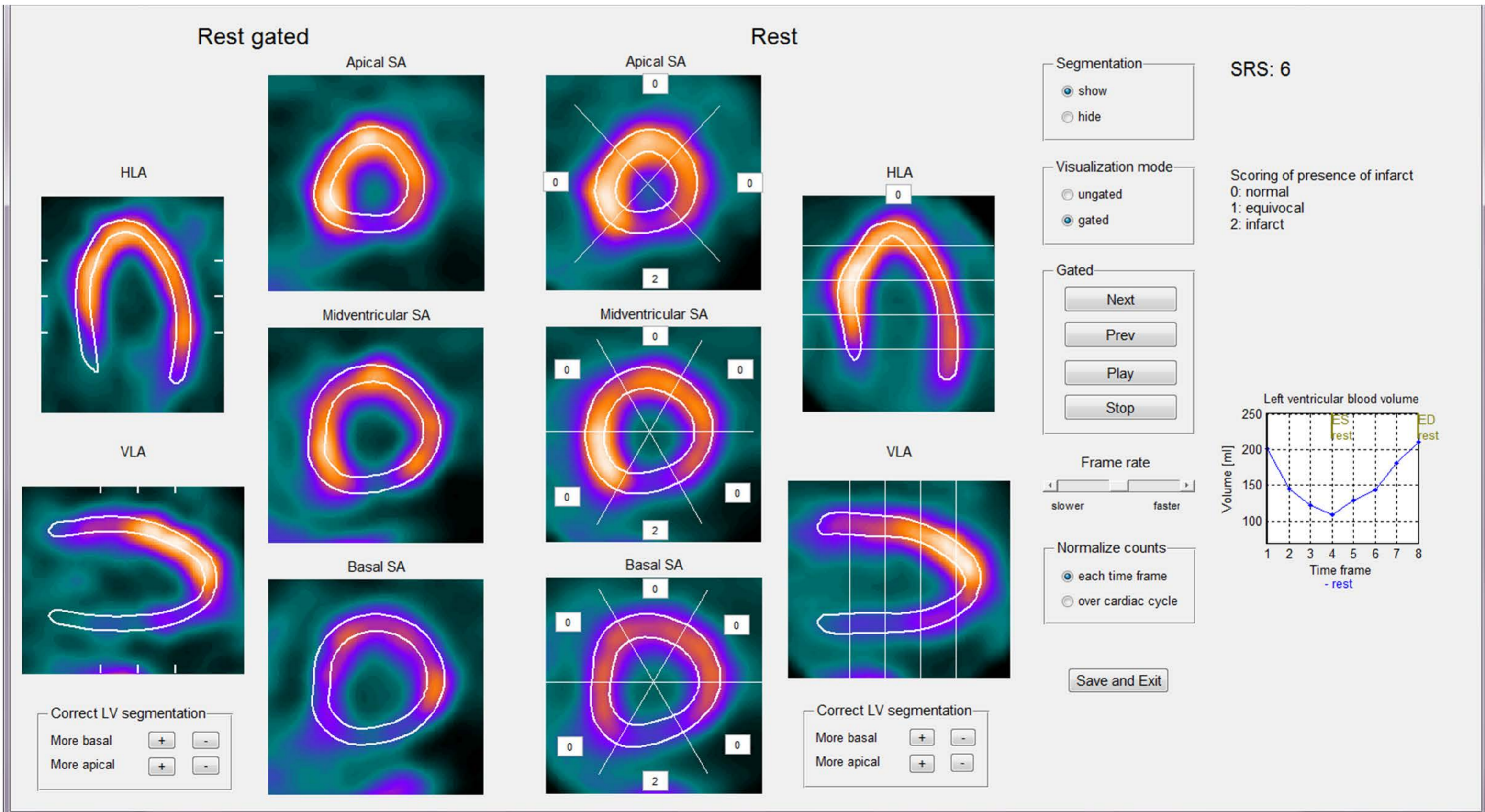
Basal SA



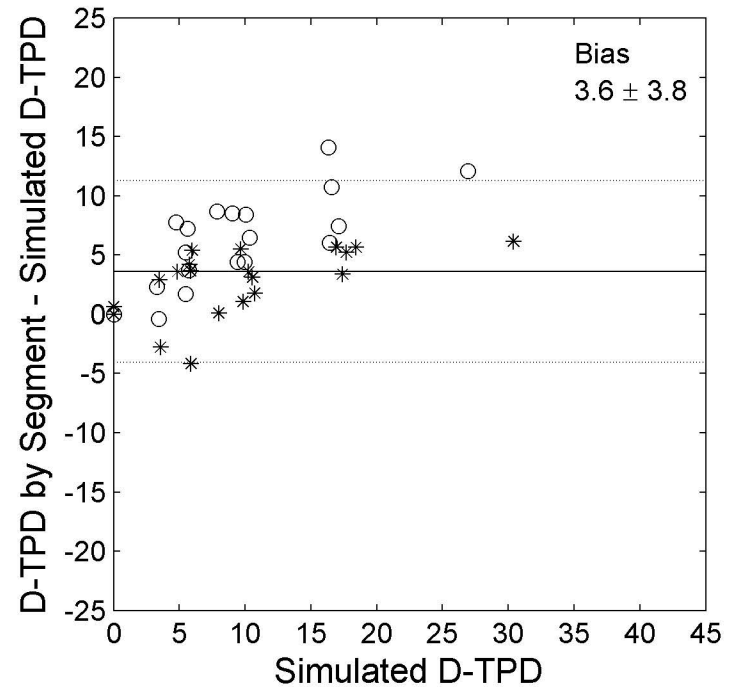
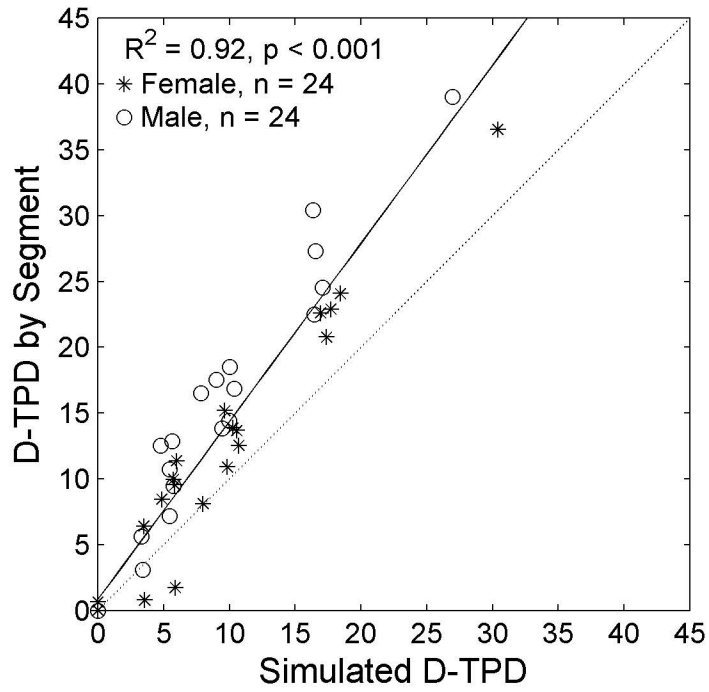
A



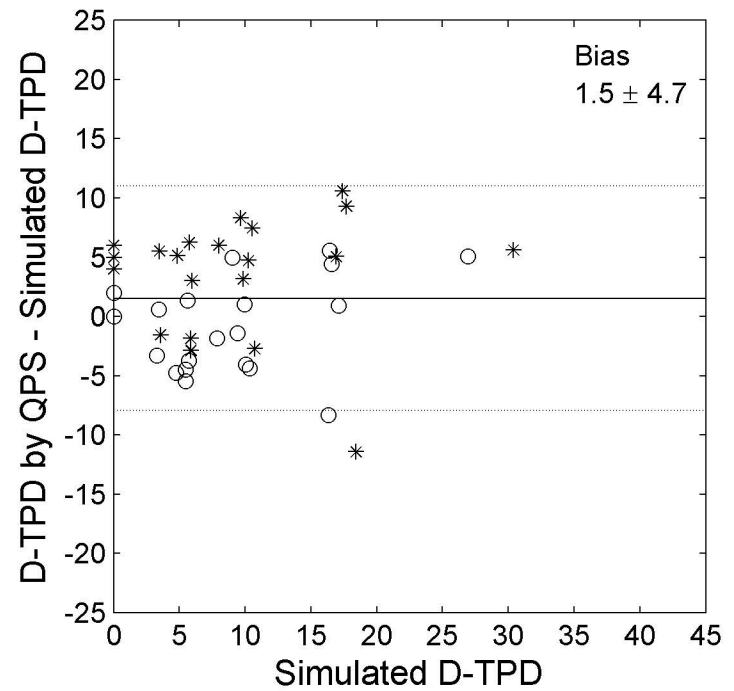
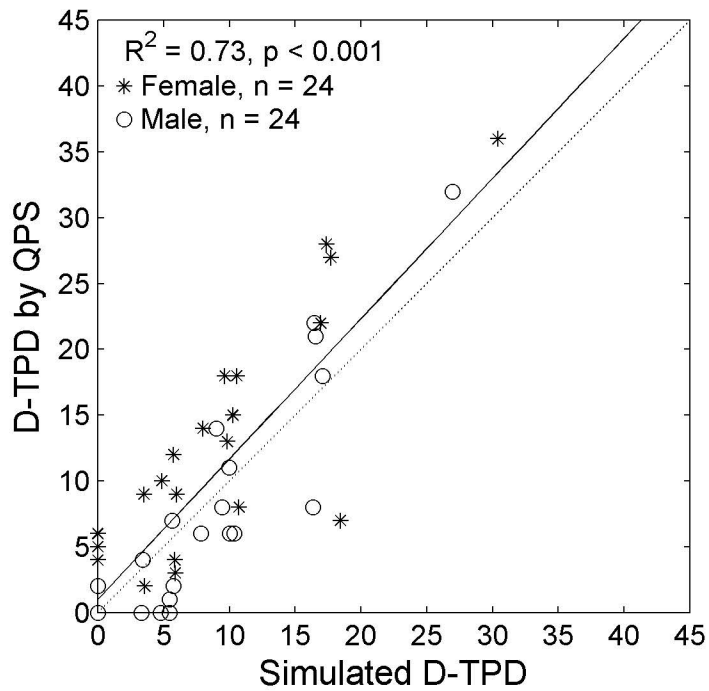
B



## SEGMENT

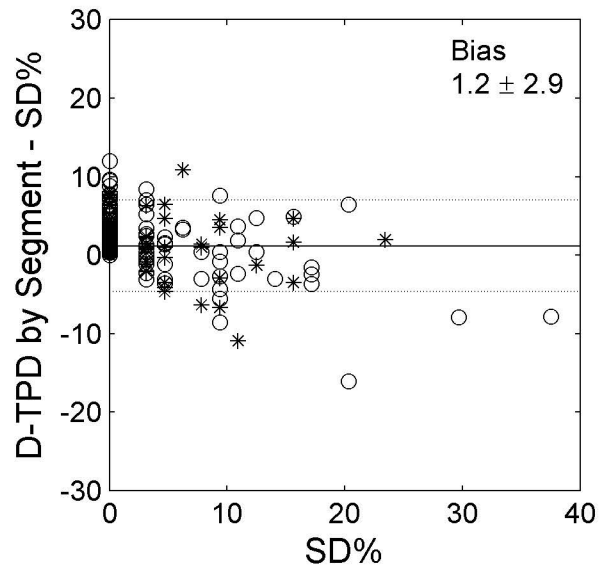
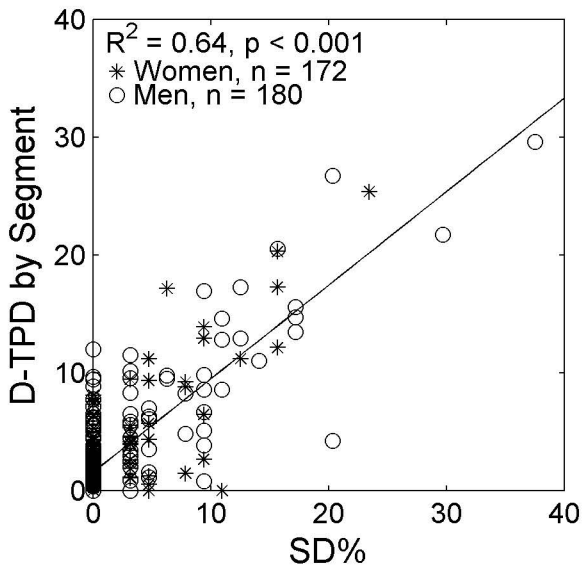


## QPS

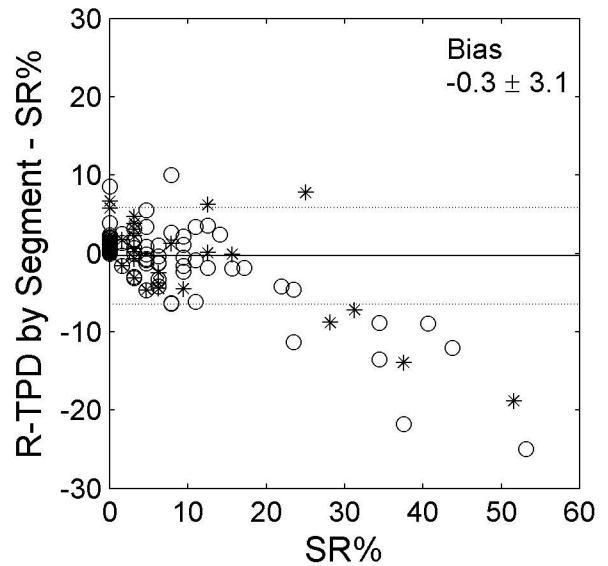
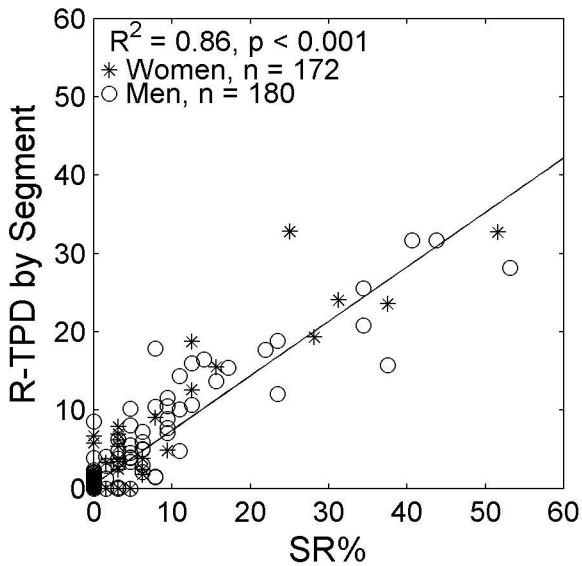


# SEGMENT

## Stress-induced ischemia

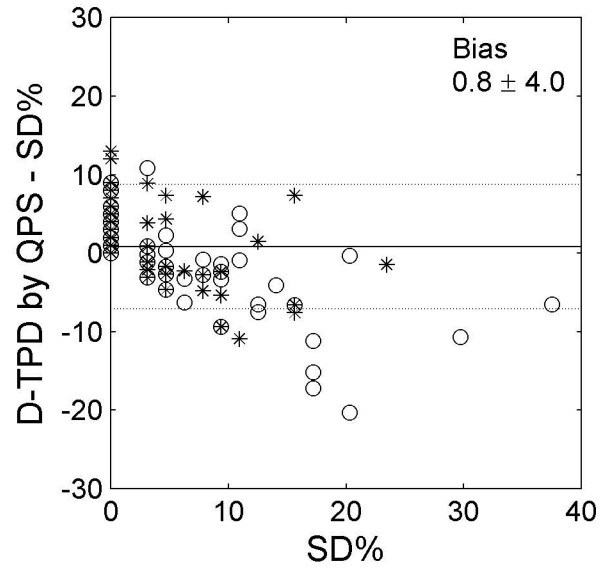
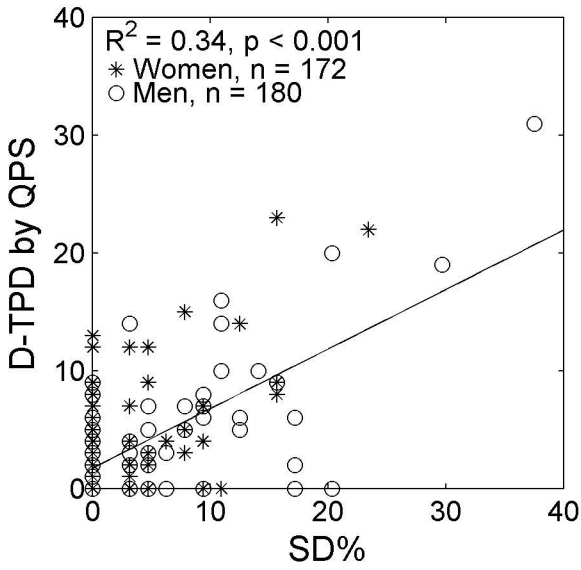


## Infarction

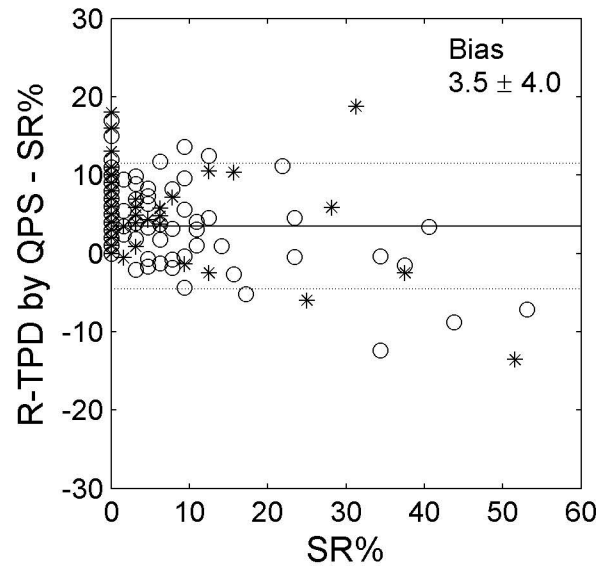
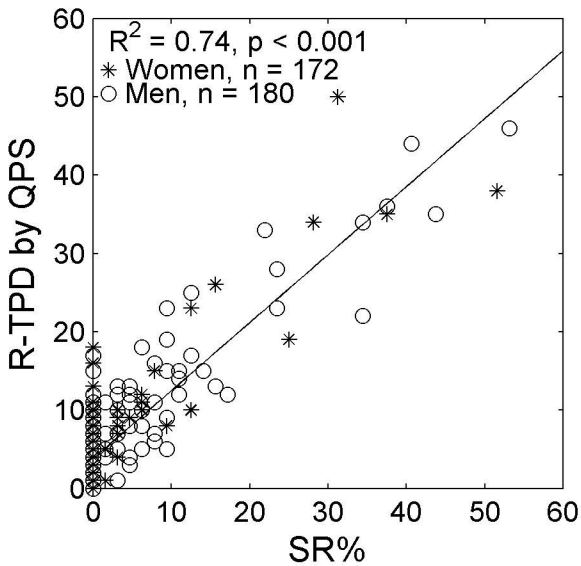


# QPS

## Stress-induced ischemia

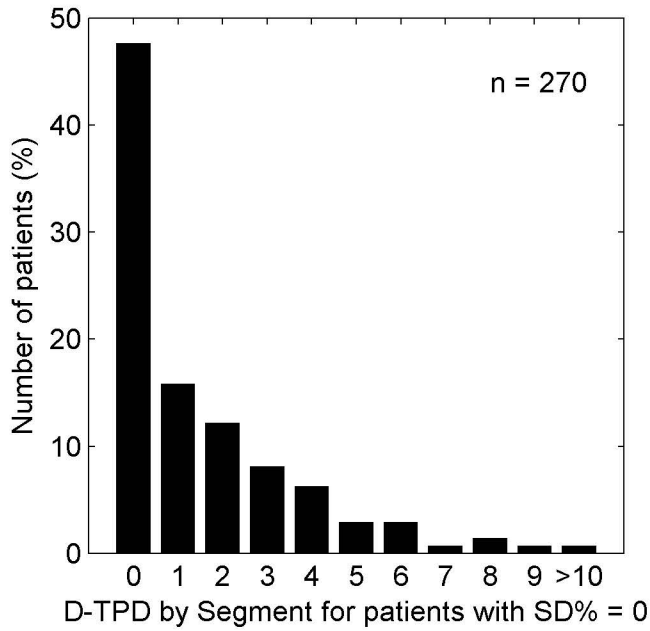


## Infarction

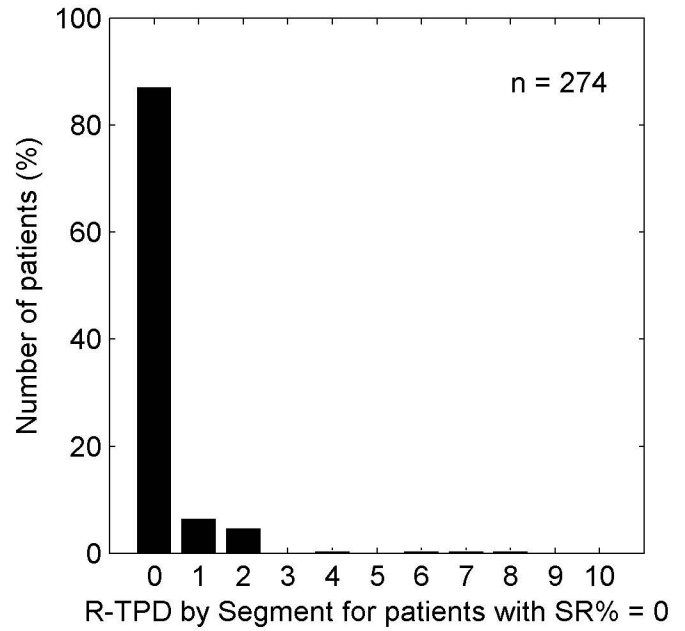


# SEGMENT

## Stress-induced ischemia

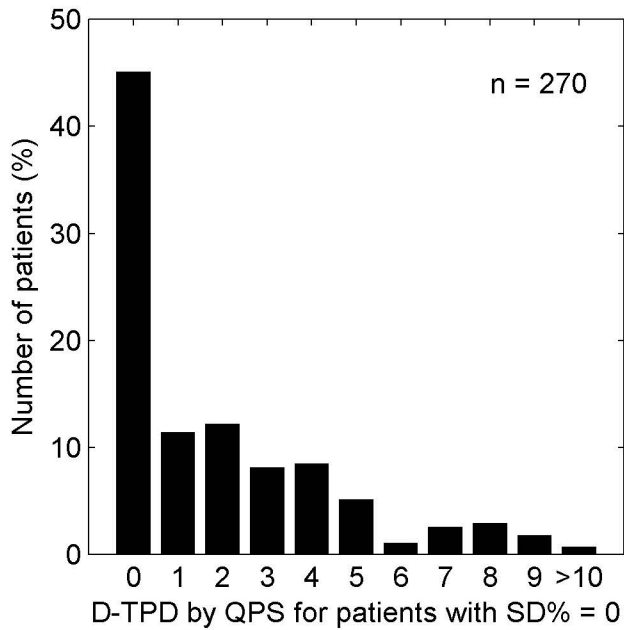


## Infarction

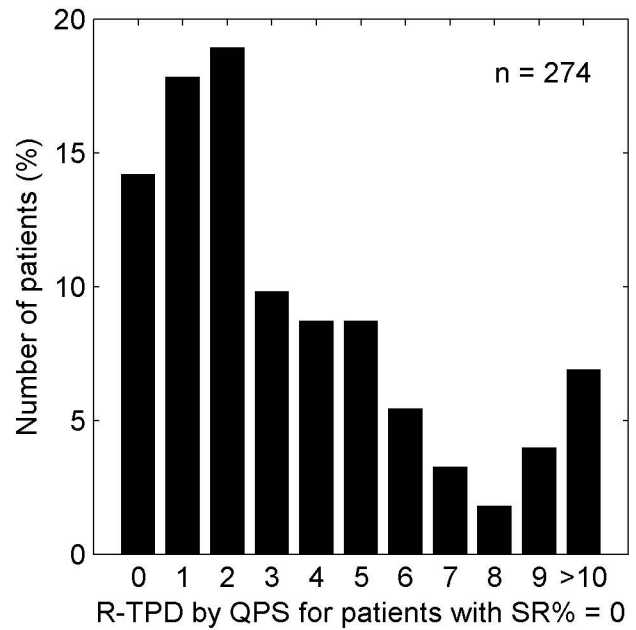


# QPS

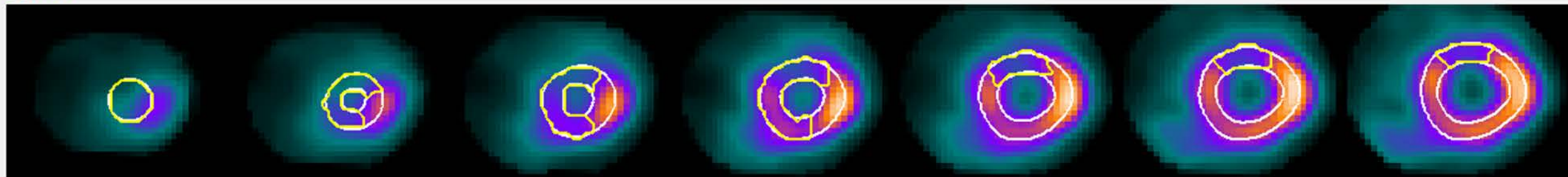
## Stress-induced ischemia



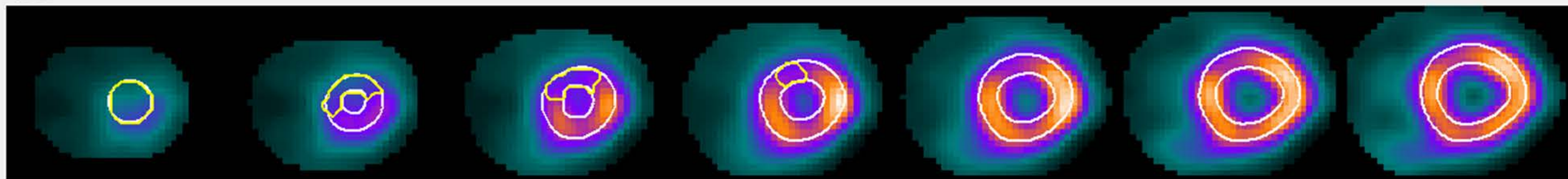
## Infarction



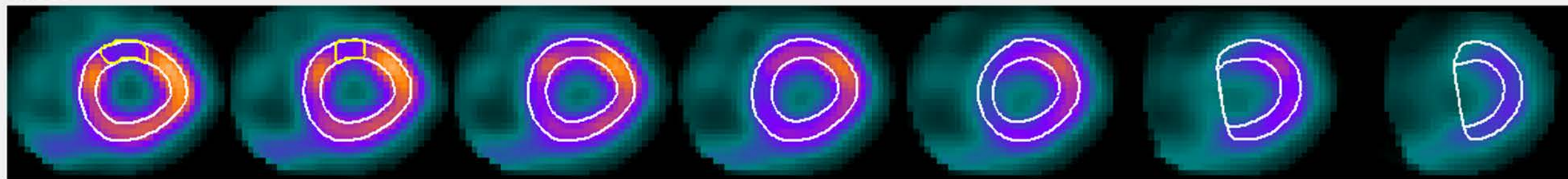
Stress



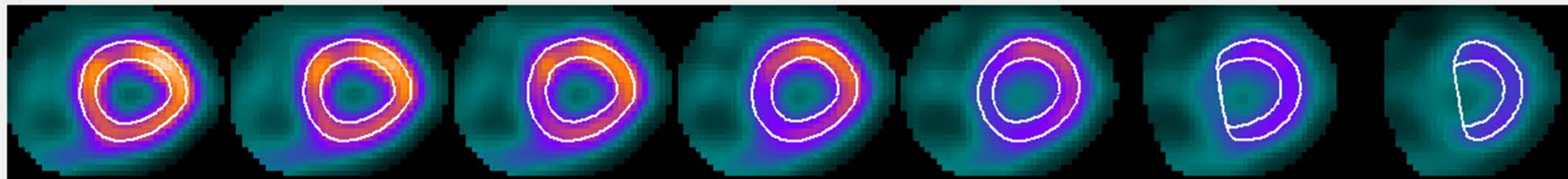
Rest



Stress



Rest

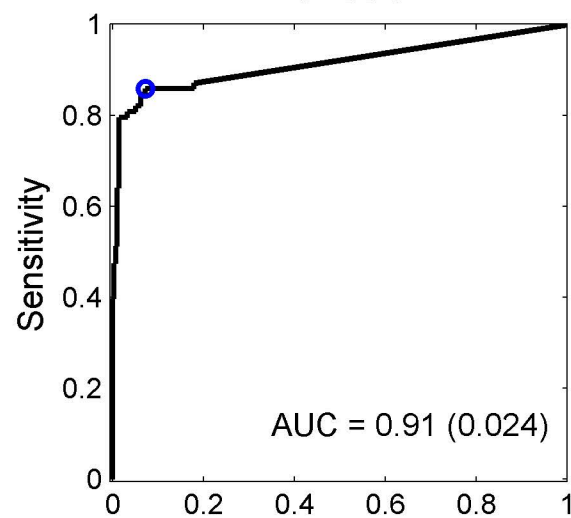
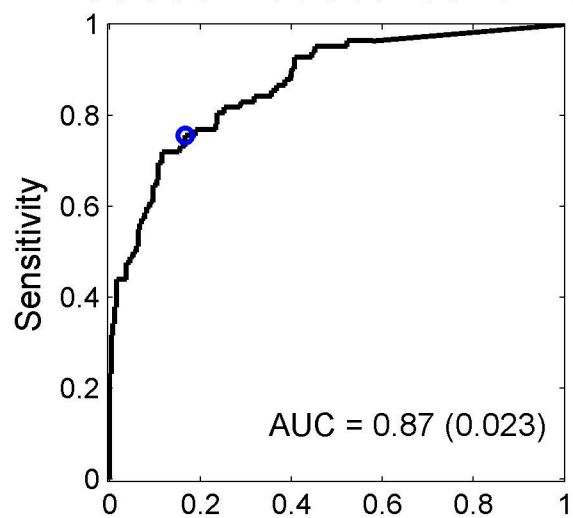


# SEGMENT

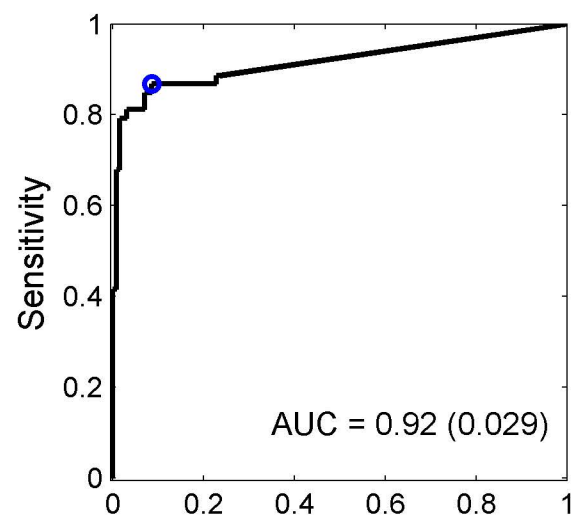
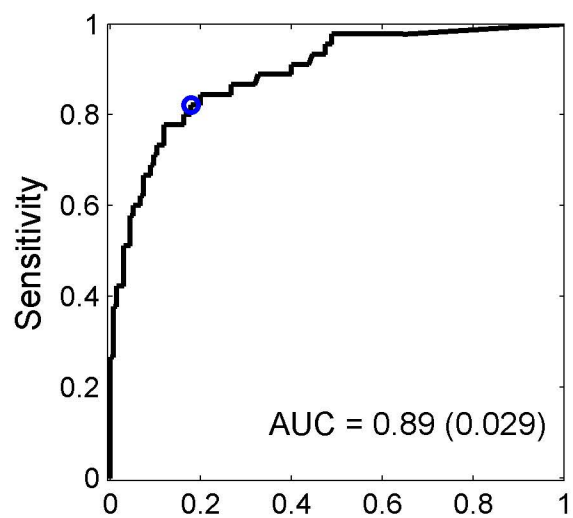
## Stress-induced ischemia

## Infarction

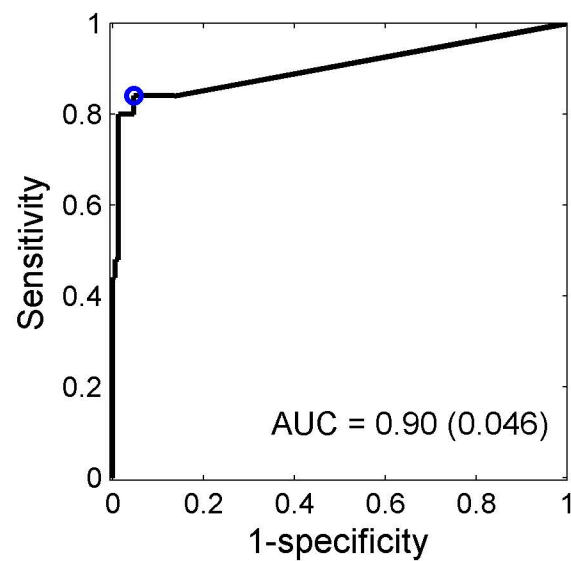
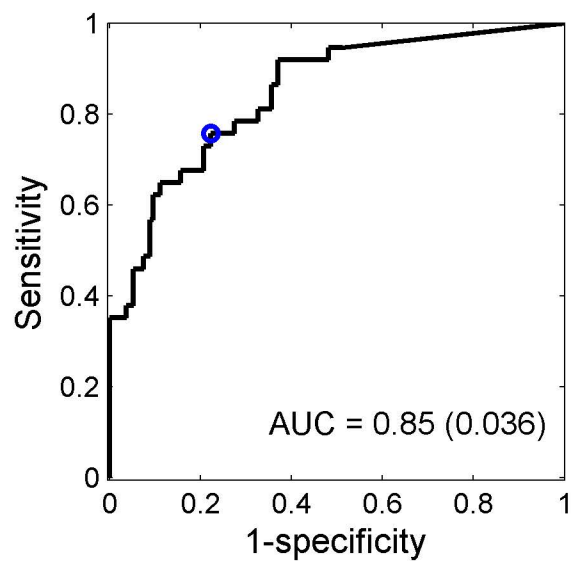
All



Men

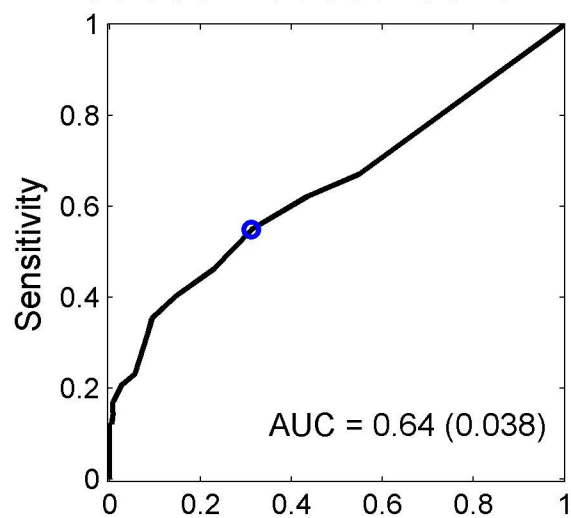


Women

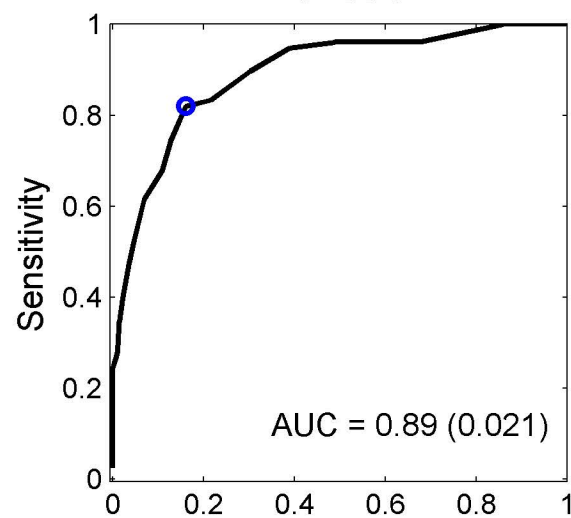


# QPS

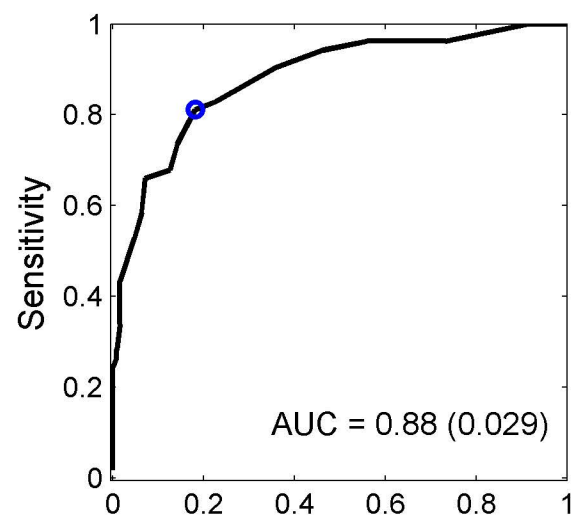
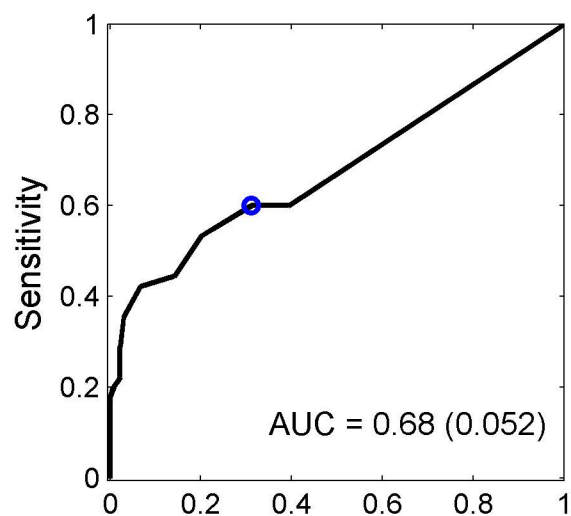
## Stress-induced ischemia



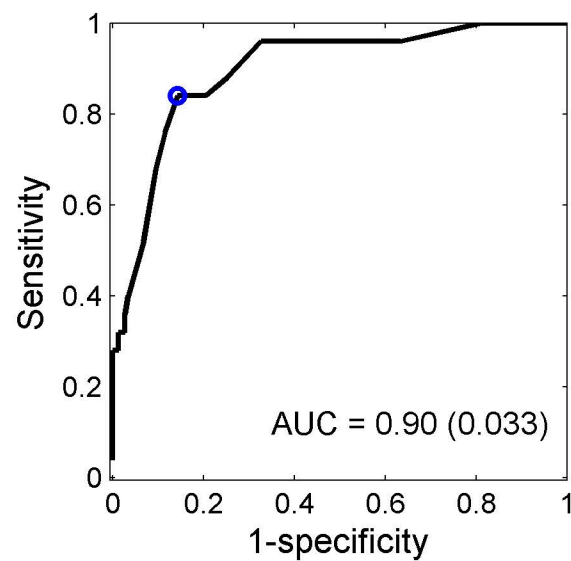
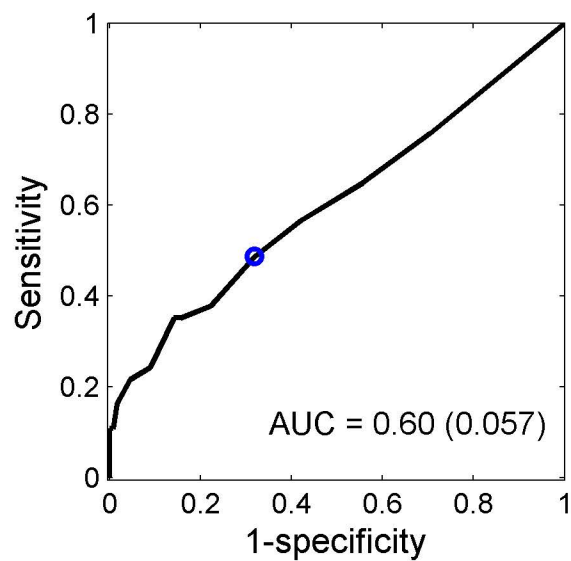
## Infarction



All



Men



Women